

# Review on Double Beta Decay Experiments & Comparison with Theory \*

Angel Morales<sup>a</sup>

<sup>a</sup>Laboratory of Nuclear Physics and High Energy Physics. Faculty of Science, University of Zaragoza, Pedro Cerbuna 12, 50009 Zaragoza, Spain

## 1. INTRODUCTION & MOTIVATION

In the Standard Model of Particle Physics neutrinos are strictly massless, although there is no theoretical reason for such prejudice. On the experimental side, there is not yet conclusive evidence that the neutrino has a non-zero mass, although the results of several experiments (widely reported to this Conference) with solar, atmospheric and terrestrial neutrinos lead to inconsistencies in the standard theory, unless it is assumed that neutrinos have indeed masses. Moreover, galaxy formation requires hot (as well as cold) non-baryonic dark matter to match properly the observed spectral power at all scales of the universe. A light neutrino of a few eV could make the hot dark matter, and help to solve the neutrino oscillation problem.

In the Standard Model, neutrinos and antineutrinos are supposed to be different particles, but no experimental proof has been provided so far. The nuclear double beta decay addresses both questions: whether the neutrino is self-conjugated and whether it has a Majorana mass. In fact, the lepton number violating neutrinoless double beta decay  $(A, Z) \rightarrow (A, Z+2) + 2e^-$  is the most direct way to determine if neutrinos are Majorana particles. For this non-standard  $2\beta 0\nu$  process to happen, the emitted neutrino in the first neutron decay must be equal to its antineutrino and match the helicity of the neutrino absorbed by the second neutron. Phenomenologically that implies the presence of a mass term or a right-handed coupling. A well-known argument of Schechter

and Valle [1] shows that in the context of any gauge theory, whatever mechanism be responsible for the neutrinoless decay, a Majorana neutrino mass is required. Moreover [23], the observation of a  $2\beta 0\nu$  decay implies a lower bound for the neutrino mass, i.e. at least one neutrino eigenstate has a non-zero mass.

Another form of neutrinoless decay,  $(A, Z) \rightarrow (A, Z+2) + 2e^- + \chi$  may reveal also the existence of the Majoron ( $\chi$ ), the Goldstone boson emerging from the spontaneous symmetry breaking of B-L, of most relevance in the generation of Majorana neutrino masses and of far-reaching implications in Astrophysics and Cosmology.

These and other issues, like the verification of SUSY models, compositeness, leptoquarks, etc. make the search for the neutrinoless double beta decay an invaluable exploration of non-standard model physics, probing mass scales well above those reached with accelerators. In this overview we will refer basically to the question of the neutrino mass in connection with the current results of the double beta decay searches.

The two-neutrino decay mode  $(A, Z) \rightarrow (A, Z+2) + 2e^- + 2\bar{\nu}_e$  is a conventional [2], although rare, second order weak process ( $2\beta 2\nu$ ), allowed within the Standard Model. The half-lives are customary expressed as  $[T_{1/2}^{2\nu}(0^+ \rightarrow 0^+)^{-1} = G_{2\nu} |M_{GT}^{2\nu}|^2]$ , where  $G_{2\nu}$  is an integrated kinematical factor [3] and  $M_{GT}^{2\nu}$  the nuclear double Gamow Teller matrix element.

The neutrinoless decay half-life (as far as the mass term contribution is concerned) is expressed as  $(T_{1/2}^{0\nu})^{-1} = F_N <m_\nu>^2 / m_e^2$ , where  $F_N \equiv G_{0\nu} |M^{0\nu}|^2$  is a nuclear factor-of-merit and  $M^{0\nu}$  is the neutrinoless nuclear matrix-element,  $M^{0\nu} = M_{GT}^{0\nu} - (g_V/g_A)^2 M_F^{0\nu}$ , with  $M_{GT,F}^{0\nu}$  the

\*Invited Review talk given at the *XVIII Intl. Conference on Neutrino Physics and Astrophysics*, Neutrino 98, Takayama (Japan), June 1998. To be published in Nucl. Phys. B (Proc. Suppl.). Ed. by Y. Suzuki, Y. Totsuka.

corresponding Gamow-Teller and Fermi contributions.  $G_{0\nu}$  is an integrated kinematic factor [3]. The quantity  $\langle m_\nu \rangle = \sum \lambda_j m_j U_{ej}^2$  is the so-called effective neutrino mass parameter, where  $U_{ej}$  is a unitary matrix describing the mixing of neutrino mass eigenstates to electron neutrinos,  $\lambda_j$  a CP phase factor, and  $m_j$  the neutrino mass eigenvalue.

As far as the neutrinoless decay with the emission of Goldstone bosons is concerned, various Majoron models have been invented to circumvent the  $Z^0$  width constrain on the number of neutrino species—which ruled out the original Majoron models—and to allow, at an observable rate, double beta neutrinoless decays with Majoron (or other massless or light bosons) emission ( $2\beta 0\nu\chi$ ). The ( $0\nu\chi$ ) half-life is expressed as  $T_{0\nu\chi}^{-1} = \langle g \rangle |M^{0\nu}|^2 G_{0\nu\chi}$ , where  $M^{0\nu}$  is the same matrix element as in the  $2\beta 0\nu$  and  $g$  the Majoron coupling to neutrinos ( $g\chi\bar{\nu}_e\gamma_5\nu_e$ ).

Concerning the neutrino mass question, the discovery of a  $2\beta 0\nu$  decay will tell that the Majorana neutrino has a mass equal or larger than  $\langle m_\nu \rangle = m_e/(F_N T_{1/2}^{0\nu})^{1/2}$  eV, where  $T_{1/2}^{0\nu}$  is the neutrinoless half life. On the contrary, when only a lower limit of the half-life is obtained (as it is the case up to now), one gets only an upper bound on  $\langle m_\nu \rangle$ , but not an upper bound on the masses of any neutrino. In fact,  $\langle m_\nu \rangle_{exp}$  can be much smaller than the actual neutrino masses. The  $\langle m_\nu \rangle$  bounds depend on the nuclear model used to compute the  $2\beta 0\nu$  matrix element. The  $2\beta 2\nu$  decay half-lives measured till now constitute bench-tests to verify the reliability of the nuclear matrix element calculations which, obviously, are of paramount importance to derive the Majorana neutrino mass upper limit.

## 2. STRATEGIES FOR DOUBLE BETA DECAY SEARCHES

The experimental signatures of the nuclear double beta decays are in principle very clear: In the case of the neutrinoless decay, one should expect a peak (at the  $Q_{2\beta}$  value) in the two-electron summed energy spectrum, whereas two continuous spectra (each one of well-defined shape) will feature the two-neutrino and the Majoron-

neutrinoless decay modes (the first having a maximum at about one third of the  $Q$  value, and the latter shifted towards higher energies). In spite of such characteristic imprints, the rarity of the processes under consideration make very difficult their identification. In fact, double beta decays are very rare phenomena, with two-neutrino half-lives as large as  $10^{19}$  y to  $10^{24}$  y and with neutrinoless half-lives as long as  $10^{25}$  y (and above), as the best lower limit stands by now. Such remotely probable signals have to be disentangled from a (much bigger) background due to natural radioactive decay chains, cosmogenic-induced activity, and man-made radioactivity, which deposit energy on the same region where the  $2\beta$  decays do it but at a faster rate. Consequently, the main task in  $2\beta$ -decay searches is to diminish the background as much as possible by going underground and using state-of-the-art ultralow background techniques to suppress it or to identify it and subtract it. All the experiments follow this general strategy because the experimental sensitivity in  $2\beta$  decay searches is limited by the level of background achieved.

To measure  $2\beta$  decays, three general approaches have been followed: The geochemical experiments, where isotopic anomalies in noble gases daughter of  $2\beta$  decaying nucleus over geological time scales are looked for. Some examples are the decays of  $^{82}\text{Se}$ ,  $^{96}\text{Zr}$ ,  $^{128}\text{Te}$ ,  $^{130}\text{Te}$ . Another method is that of the radiochemical experiments, which are based on the fact that when the daughter nuclei of a double beta emitter are themselves radioactive, they can be accumulated, extracted and counted. Examples are  $^{238}\text{U}$ ,  $^{244}\text{Pu}$ .

Most of the recent activity, however, refers to direct counting experiments, which measure the energy of the  $2\beta$  emitted electrons and so the spectral shapes of the  $2\nu$ ,  $0\nu$ , and  $0\nu\chi$  modes of double beta decay. Some experimental devices track also the electrons (and other charged particles), measuring the energy, angular distribution, and topology of events. The tracking capabilities are essential to discriminate the  $2\beta$  signal from the background. The types of detectors currently used are:

- Calorimeters where the detector is also the  $2\beta$  source (Ge diodes, scintillators— $\text{CaF}_2$ ,  $\text{CdWO}_4$ —, thermal detectors, ionization chambers). They are calorimeters which measure the two-electron sum energy and discriminate partially signal from background by pulse shape analysis (PSD).
- Tracking detectors of source $\neq$ detector type (Time Projection Chambers TPC, drift chambers, electronic detectors). In this case, the  $2\beta$  source plane(s) is placed within the detector tracking volume, defining two—or more—detector sectors.
- Tracking calorimeters: They are tracking devices where the tracking volume is also the  $2\beta$  source. Only one of this type of device is operating (a Xenon TPC), but there are others in project.

Well-known examples of  $2\beta$  emitters measured in direct counting experiments are  $^{48}\text{Ca}$ ,  $^{76}\text{Ge}$ ,  $^{96}\text{Zr}$ ,  $^{82}\text{Se}$ ,  $^{100}\text{Mo}$ ,  $^{116}\text{Cd}$ ,  $^{130}\text{Te}$ ,  $^{136}\text{Xe}$ ,  $^{150}\text{Nd}$ .

The strategies followed in the  $2\beta$  searches are varied. Calorimeters of good energy resolution and almost 100% efficiency (Ge-detectors, Bolometers) are well suited for  $0\nu$  searches. However, they lack the tracking capabilities to identify the background on an event-by-event basis. Pulse Shape Discrimination (PSD) will help. Simultaneous measure of heat and ionization would do it. The Monte Carlo (MC) modeling of the background spectrum to be subtracted from the data is approximate. So, one should first reduce the radioimpurities as much as possible and then trace back and MC-model the remaining contaminations and subtract them. On the contrary, the identification capabilities of the various types of chambers make them very well suited for  $2\nu$  and  $0\nu\chi$  searches. However, their energy resolution is rather modest and the efficiency is only of a few percent. Furthermore, the ultimate major background source in these devices when looking for  $2\beta 0\nu$  decay will be that due to the standard  $2\beta 2\nu$  decay. The rejection of background provided by the tracking compensates, however, the figure of merit in  $0\nu$  searches. Modular calorimeters can have large amounts of  $2\beta$  emitters (Hei-

delberg/Moscow, IGEX, CUORE and GENIUS project). However, current operating chambers—except the Xe/TPC—cannot accommodate large amounts of  $2\beta$  emitters in the source plate. Future tracking devices will have 10 kg and more (NEMO3, MUNU).

As a general rule, the detector must optimize the so-called detector factor-of-merit or neutrinoless sensitivity (introduced by the pioneer work of E. Fiorini), which for source=detector devices reads  $F_D = 4.17 \times 10^{26} (f/A)(Mt/B\Gamma)^{1/2} \varepsilon_\Gamma$  years where B is the background rate (c/keV kg y), M the mass of  $2\beta$  emitter (kg),  $\varepsilon_\Gamma$  the detector efficiency in the energy bin  $\Gamma$  around  $Q_{2\beta}$  ( $\Gamma = \text{FWHM}$ ) and t the time measurement in years (f is the isotopic abundance and A the mass number). The other guideline of the experimental strategy is to choose a  $2\beta$  emitter of large nuclear factor of merit  $F_N = G_{0\nu} |M^{0\nu}|^2$ , where the kinematical factor qualifies the goodness of the  $Q_{2\beta}$  value and  $M^{0\nu}$  the likeliness of the transition. Notice that the upper limit on  $\langle m_\nu \rangle$  is given by  $\langle m_\nu \rangle < m_e / (F_D F_N)^{1/2}$ .

### 3. OVERVIEW OF EXPERIMENTAL SEARCHES

In the following we will overview some of the direct counting experiments, reporting only on  $2\beta$  transitions to the ground state. A considerable activity has been done recently on transitions to excited states but we will omit them for lack of space.

There exist two experiments in operation looking for the double beta decay of  $^{76}\text{Ge}$ . They both employ large amounts of enriched  $^{76}\text{Ge}$  in sets of detectors. The Heidelberg/Moscow Collaboration experiment (a set of five large Ge detectors amounting to 10.2 kg) running in Gran Sasso [4] (exposed by H.V. Klapdor-Kleingrothaus in these Proceedings), and the IGEX Collaboration in Canfranc (Spain), which is described below.

The International Germanium Experiment (IGEX) has three large enriched (up to 86%) detectors ( $\sim 2$  kg) and three smaller ones ( $\sim 1$  kg). The FWHM energy resolutions of the large detectors at 1333-keV are 2.16, 2.37, and 2.13 keV, and the energy resolution of the summed data is

Table 1

Theoretical half-lives  $T_{1/2}^{2\nu}$  in some representative nuclear models versus direct experiments.

	<i>Theory</i>								<i>Experiment</i>	
	SM			QRPA		$1^+D$	OEM	MCM		
	[2]	[12]	[13]	[14]	[16]	[19]	[18]	[17]		
$^{48}\text{Ca}(10^{19}\text{y})$	2.9	7.2	3.7						4.3	$^{+2.4}_{-1.1} \pm 1.4$ UCI
$^{76}\text{Ge}(10^{21}\text{y})$	0.42	1.16	2.2	1.3	3.0		0.28	1.9	1.77	$^{+0.14}_{-0.12}$ H/M 1.45 $\pm 0.15$ IGEX
$^{82}\text{Se}(10^{20}\text{y})$	0.26	0.84	0.5	1.2	1.1	2.0	0.88	1.1	1.08	$^{+0.26}_{-0.06}$ UCI 0.83 $\pm 0.09 \pm 0.06$ NEMO
$^{96}\text{Zr}(10^{19}\text{y})$				0.85	1.1			.14-.96	2.1	$^{+0.8}_{-0.4} \pm 0.2$ NEMO
$^{100}\text{Mo}(10^{19}\text{y})$				0.6	0.11	1.05	3.4	0.72	1.15	$^{+0.30}_{-0.20}$ Osaka 1.16 $^{+0.34}_{-0.08}$ UCI 0.95 $\pm 0.04 \pm 0.09$ NEMO
$^{116}\text{Cd}(10^{19}\text{y})$					6.3	0.52		0.76	2.6	$^{+0.9}_{-0.5}$ Osaka 2.7 $^{+0.5}_{-0.4} \pm 0.9 \pm 0.6$ Kiev 3.75 $\pm 0.35 \pm 0.21$ NEMO
$^{136}\text{Xe}(10^{21}\text{y})$		2.0	0.85	4.6						$\geq 0.55$ Gothard
$^{150}\text{Nd}(10^{19}\text{y})$					0.74				1.88	$^{+0.66}_{-0.39} \pm 0.19$ ITEP 0.675 $^{+0.037}_{-0.042} \pm 0.068$ UCI

4 keV (at the  $Q_{2\beta}$  value of 2038 keV). They feature a unique electroformed copper technology in the cryostat and use ultralow background materials. The first stage FET (mounted on a Teflon block a few centimetres apart from the centre contact of the crystal) is shielded by 2.6 cm of 500 y old lead to reduce the background. Also the protective cover of the FET and the glass shell of the feedback resistor were removed for such purpose. Further stages of amplification are located 70 cm away from the crystal. All the detectors have preamplifiers modified for pulse shape analysis (PSD) for background identification.

The Canfranc IGEX setup consists in an innermost shield of 2.5 tons ( $\sim 60$  cm cube) of archaeo-

logical lead (2000 yr old)—having a  $^{210}\text{Pb}$ ( $^{210}\text{Bi}$ ) content of  $< 0.01$  Bq/kg—, where the 3 large detectors are fitted into precision-machined holes to minimize the empty space around the detectors available to radon. Nitrogen gas evaporated from liquid nitrogen, is forced into the remaining free space to minimize radon intrusion. Surrounding the archaeological lead block there is a 20-cm thick layer of low activity lead ( $\sim 10$  tons), sealed with plastic and cadmium sheets. A cosmic muon veto and a neutron shield close the assembly.

The background recorded in the energy region between 2.0 and 2.5 MeV is about 0.2 c/keV kg y prior to PSD. Background reduction through pulse shape discrimination is in progress to elim-

inate multisite events, characteristic of non- $2\beta$  events. This technique is currently capable of rejecting about one third of the background events, so the current IGEX background is  $\leq 0.07$  c/keV kg y. Further preamplifier development and pulse shape simulations are expected to improve the background rejection efficiency, pursuing the goal of probing Majorana neutrino masses corresponding to half-lives of  $10^{26}$  years. The current results of IGEX, both for the  $2\beta 2\nu$  and  $2\beta 0\nu$  decay modes, are given in Tables 1 and 2. The two-electron summed energy spectrum around  $Q_{2\beta} = 2038$  keV region is shown in Figure 1 for an exposure of 92.68 mole years. Data from one of the large detectors—which went underground in Canfranc more than three years ago—corresponding to 291 days, were used to set a value for the  $2\nu$ -decay mode half-life by simply subtracting MC-simulated background. Figure 2a shows the best fit to the stripped data corresponding to a half-life  $T_{1/2}^{2\nu} = (1.45 \pm 0.20) \times 10^{21}$  y, whereas Figure 2b shows how the experimental points fit the double beta Kurie plot.

Table 2  
Limits on Neutrinoless Decay Modes

<i>Emitter</i>	<i>Experiment</i>	$T_{1/2}^{0\nu}$	<i>C.L.</i>
$^{48}\text{Ca}$	HEP Beijing	$> 1.1 \times 10^{22}$ y	68%
$^{76}\text{Ge}$	MPIH/KIAE	$> 1.2 \times 10^{25}$ y	90%
	IGEX	$> 0.8 \times 10^{25}$ y	90%
$^{82}\text{Se}$	UCI	$> 2.7 \times 10^{22}$ y	68%
	NEMO 2	$> 9.5 \times 10^{21}$ y	90%
$^{96}\text{Zr}$	NEMO 2	$> 1.3 \times 10^{21}$ y	90%
$^{100}\text{Mo}$	LBL/MHC/	$> 2.2 \times 10^{22}$ y	68%
	UNM		
	UCI	$> 2.6 \times 10^{21}$ y	90%
	Osaka	$> 2.8 \times 10^{22}$ y	90%
$^{116}\text{Cd}$	NEMO 2	$> 6.4 \times 10^{21}$ y	90%
	Kiev	$> 3.2 \times 10^{22}$ y	90%
	Osaka	$> 2.9 \times 10^{21}$ y	90%
	NEMO 2	$> 5 \times 10^{21}$ y	90%
$^{130}\text{Te}$	Milano	$> 7.7 \times 10^{22}$ y	90%
$^{136}\text{Xe}$	Caltech/UN/	$> 4.4 \times 10^{23}$ y	90%
	PSI		
$^{150}\text{Nd}$	UCI	$> 1.2 \times 10^{21}$ y	90%

The Time Projection Chamber TPC of the UC Irvine group is a rectangular box filled with helium and located underground at 290 m.w.e. (Hoover Dam). A central  $2\beta$  source plane divides the volume into two halves. A magnetic field of 1200 Gauss is placed perpendicular to the source plane. Electrons emitted from the source follow helical trajectories from where the momentum and the angles of the  $\beta$ -particles are determined. The  $2\beta$  signal is recognized as two electron emitted from a common point in the source with no other associated activity during some time before and after the event. The  $2\beta$  source is thin enough (few mg/cm<sup>2</sup>) to allow  $\alpha$ -particles to escape and be detected for tagging the background. The UCI TPC has measured the two-neutrino double beta decay of  $^{82}\text{Se}$ ,  $^{100}\text{Mo}$ ,  $^{150}\text{Nd}$  and  $^{48}\text{Ca}$  (this last case in a collaboration with Caltech and the Kurchatov Institute), with efficiencies of about  $\sim 11\%$  and energy resolution of  $\sim 10\%$  at the Q value. Figures 3.1, 3.2 and 3.3 show respectively [5] the UCI  $2\beta 2\nu$  decay spectra of  $^{100}\text{Mo}$ ,  $^{150}\text{Nd}$  and  $^{48}\text{Ca}$ , depicting in each case the measured spectra and their background components as well as the corresponding  $2\beta$ -decay best fits. Results are quoted in Tables 1 and 2.

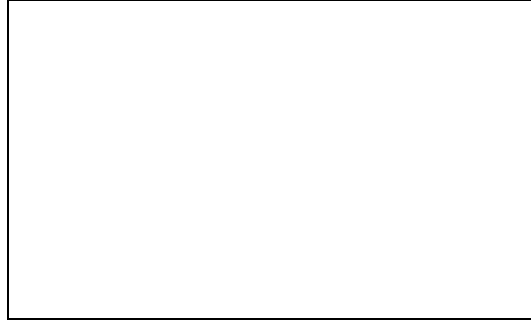


Figure 1.

The NEMO 2 apparatus [6] is an electron tracking detector (with open Geiger cells) filled with helium gas. An external calorimeter (plastic scin-

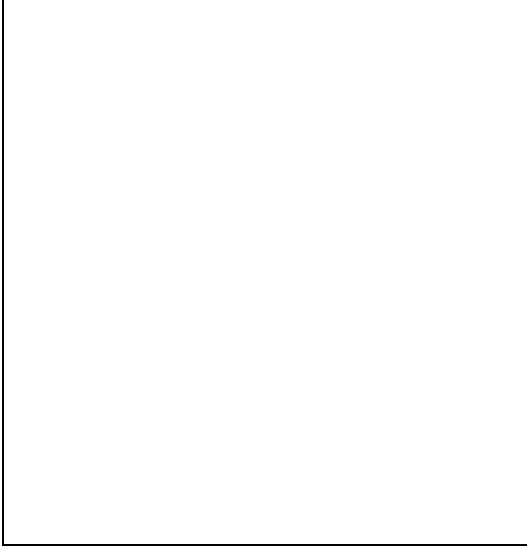


Figure 2.

tillator) covers the tracking volume and measures the  $\beta$  energies and time of flight. The  $2\beta$  source is placed in a central vertical plane and is divided in two halves, one enriched and another of natural abundance (of about 150 grams each), to monitor and subtract the background. To identify a  $2\beta$  signal, one should have a 2e-track with a common vertex ( $\cos\alpha < 0.6$ ) in the source plus two fired plastic scintillators (E deposition  $> 200$  keV each). The two-electron events are selected by time of flight analysis (in the energy range of  $2\beta$ ). NEMO 2 has been operating for several years at the Modane Underground Laboratory (Frejus Tunnel) at 4800 m.w.e and has measured the  $2\beta 2\nu$  decays of  $^{100}\text{Mo}$ ,  $^{116}\text{Cd}$ ,  $^{82}\text{Se}$  and  $^{96}\text{Zr}$  (see Figures 4a,b,c,d) with an efficiency of about  $\varepsilon_{2\nu} \sim 2\%$  and an energy resolution  $\Gamma$  (1 MeV) = 18% (for results refer to Table 1 and Table 2). A new, bigger detector of the NEMO series, NEMO 3, is ready to start running next year, with 10 kg of  $^{100}\text{Mo}$ .

The ELEGANTS V detector of the University of Osaka (placed successively in Kamioka and Otho) is an electron tracking detector which con-

sists of two drift chambers for  $\beta$ -trajectories, sixteen modules of plastic scintillators for  $\beta$  energies and timing measurement, and twenty modules of NaI for X- and  $\gamma$ -rays identification. The  $2\beta$  signals should appear as two tracks in the drift

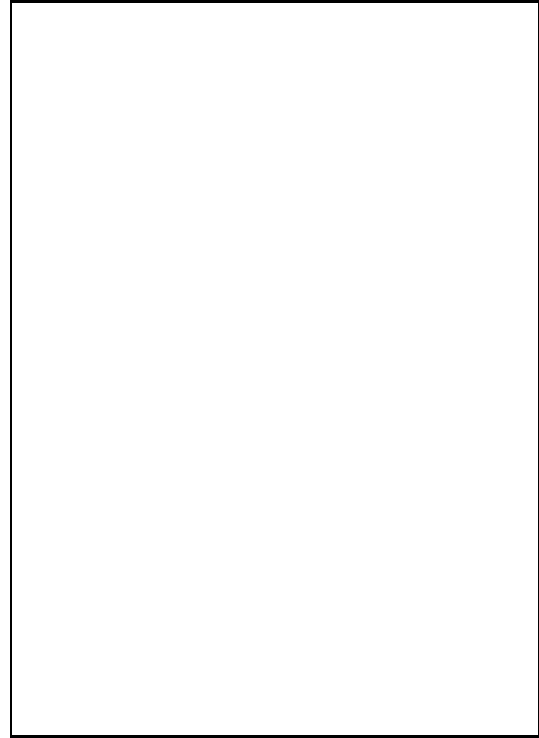


Figure 3.

chamber with the vertex in the source plus two signals from two plastic scintillators segments. Both enriched and natural sources (of about 100 grams) are employed in the detector for background monitoring and subtraction. This detector has measured [7] the  $2\beta 2\nu$  decay of  $^{116}\text{Cd}$ ,  $^{100}\text{Mo}$  (see Figure 5a,b) with efficiencies of  $\varepsilon_{2\nu} \sim 7\% \sim 10\%$  and  $\varepsilon_{0\nu} \sim 20\%$ , and energy resolution of 150 keV at 1 MeV (the results of ELEGANTS V are quoted in Tables 1 and 2). A new variant of ELEGANTS is searching for the double beta

decay of  $^{48}\text{Ca}$ .



Figure 4.

The Caltech/PSI/Neuchatel Collaboration [8] investigates the double beta decay of  $^{136}\text{Xe}$  in the Gothard Tunnel (3000 m.w.e.) by using a time projection chamber where the Xenon is at the same time the source and the detector medium, i.e. a calorimeter plus a tracking device. It has a cylindrical drift volume of 180 fiducial litres at a pressure of 5 atm. The Xenon is enriched up to 62.5% in  $^{136}\text{Xe}$ , with a total mass of  $m=3.3$  kg. The energy resolution is 6.6% at 2.48 MeV and the  $2\beta 0\nu$  efficiency  $\varepsilon_{0\nu} \sim 30\%$ . The  $2\beta$  signal appears as a continuous trajectory with distinctive end features: a large angle multiple scattering and increase charge deposition (charge “blobs”) at both ends. As usual, the  $2\beta$  topology gives powerful background rejection, leading to a figure of  $B \sim 10^{-1} - 10^{-2}$  c/keV kg y (at 2480 keV). In the neutrinoless decay mode search, the experimental set up has already reached its limit (Table 2 and Figure 6). In the two-neutrino decay mode, the comparison of the single-electron and two-electron background spectra before and after a recent upgrading [8] of the readout plane (a factor 4 reduction in single  $e^-$  background above 1800 keV) shows that the two-electron spectrum

is not reduced as much as the single-electron one. That implies that a significant  $2\beta$  signal is contained in the 2e data, and so a new run (at low pressure) is in progress in a search for the  $2\beta 2\nu$  mode.

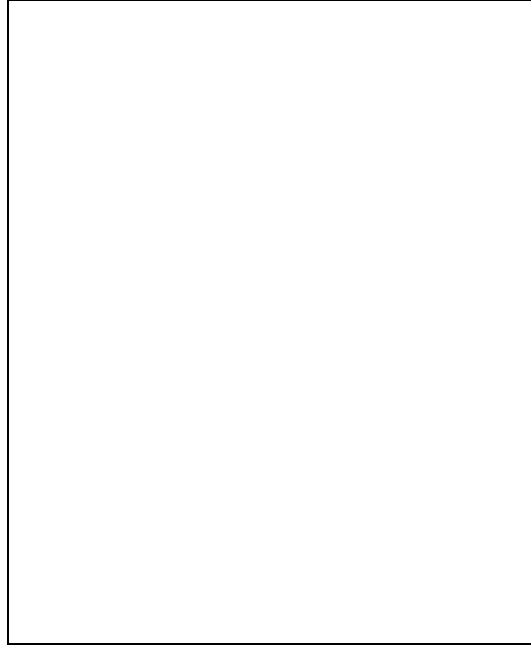


Figure 5.

The ITEP group has measured [9] the double beta decay of  $^{150}\text{Nd}$  (40 g) with a TPC of  $\sim 300$  litres filled with  $\text{CH}_4$  at atmospheric pressure, in a 700 gauss magnetic field. The detection efficiency is  $\varepsilon_{2\nu} \sim 3\%$  (see results in Table 1). A large ( $13\text{m}^3$ ) TPC is underway for Xe (7.5 kg) and Nd (5 kg).

The group of INR at Kiev [10] is investigating the double beta decay of  $^{116}\text{Cd}$  with cadmium tungstate ( $^{116}\text{CdWO}_4$ ) scintillator crystals of 12 to  $15\text{ cm}^3$  which feature an energy resolution of  $\Gamma = 7\%$  at 2614 keV. A series of test experiments to reduce the background has led to a figure of  $B \sim 0.6$  c/keV kg y. Results are quoted in Tables



Figure 6.

1 and 2.

A series of bolometer experiments have been carried out by the Milan group since 1989 in the Gran Sasso Laboratory, searching for the double beta decay of  $^{130}\text{Te}$  [11]. The increase of the temperature produced by the energy released in the crystal due to a nuclear event (i.e.  $2\beta$ ), is measured by means of a sensor in thermal contact with the absorber. The Milan group uses Tellurium oxide crystals as absorbers, and glued NTD Ge thermistors as sensors. Notice that natural Tellurium contains 34% of  $^{130}\text{Te}$ . After using successively  $\text{TeO}_2$  crystals of 73 g and 334 g, as well as a set of four of these large crystals, a tower-like array of 20 crystals of 340 g in a copper frame is currently taking data at a temperature of  $\sim 10$  mK. In a recent run, featuring an energy resolution (summed over the twenty energy spectra) of  $\sim 10$  keV at 2615 keV, and a background of about 0.5 c/keV kg day in that region, they got in only a few days a better neutrinoless half-life limit than in all their previous experiments (See Table 2). The calibration spectrum of the summed twenty-crystal spectra and the background around the  $Q_{2\beta}$  region corresponding to a short running have been presented to this Conference [11] and are

shown in Figures 7a,b. An enlarged version of this experiment, CUORE (a Cryogenic Underground Observatory for Rare Events) consisting of an array of 1000 crystals of  $\text{TeO}_2$  of 750 g each (with NTD Ge sensors), operating at  $7 \sim 10$  mK, is planned to be installed at Gran Sasso [11].

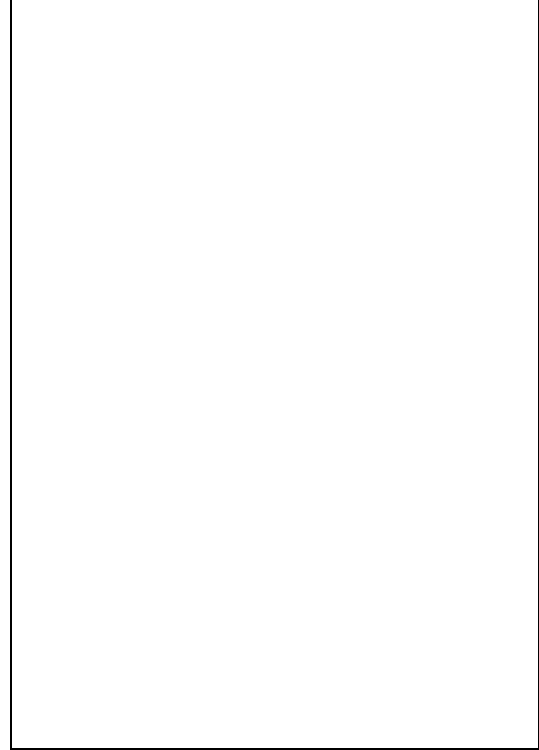


Figure 7.

#### 4. EXPERIMENTAL RESULTS CONFRONT THEORY

Two main lines have been followed in computing the  $2\beta$ -decay nuclear matrix elements: Shell Model (SM) and Quasiparticle Random Phase Approximation (QRPA). Both approaches have been widely applied with various degrees of success. The current theoretical predictions of the  $2\nu$



decay modes have provided a general framework of concordance with the experiment (within a factor 2–5). That gives confidence in the reasonable reliability of the  $2\beta 0\nu$  decay matrix elements used to extract  $\langle m_\nu \rangle$  bounds.

The first attempts to calculate  $2\beta$  nuclear matrix element were made by using the nuclear shell model, but as most  $2\beta$  emitters are heavy or medium heavy nuclei, it was necessary to use a weak coupling limit shell model [2,12] and/or truncation of the model space to cope with the calculation. Such truncations excluded configurations relevant for the final results. Predictions of such former calculations are given in Tables 1 and 3. Until recently, large SM calculations were possible only in the case of  $^{48}\text{Ca}$  [13]a. New progress in SM codes have allowed to perform large model space SM calculations [13]b in heavy and medium heavy nuclei using realistic single particle basis. Still there are important truncations because of the large valence space. For  $^{48}\text{Ca}$ ,  $^{76}\text{Ge}$  and  $^{82}\text{Se}$ , the results are in good agreement with the experiment, whereas for  $^{136}\text{Xe}$  there exists some discrepancy (See Table 1). Estimates of the neutrinoless decays in this large model space SM calculation give longer neutrinoless decay half-lives (for equal  $\langle m_\nu \rangle$  values) than the QRPA results.

QRPA is simple from a computing point of view; it includes many features of the two-body interaction which plays a relevant role in  $2\beta$  decays; it is very sensitive to the  $J = 1^+$ ,  $T = 0$  particle-particle interaction and have contributed significantly to understand the large suppression of the experimental rates which failed to be explained by the earlier theoretical approaches. QRPA was first applied to compute the  $2\beta 2\nu$  matrix elements by the Caltech group [14] using a zero range force. Results in agreement with experiment were obtained for various  $2\beta$  measured decays, when the value of the strength  $g_{pp}$  of the particle-particle interaction used was the one fitting the  $\beta^+$  decay of nuclei with magic number of neutrons. Subsequent works of the groups of Tübingen [15] and of Heidelberg [16] (both in  $2\nu$  and  $0\nu$  decays) confirmed and refined the results with more realistic NN interactions. The suppression of the  $2\beta 2\nu$  matrix elements is extremely sensitive to the strength  $g_{pp}$  of the particle-particle

interaction, which in fact may lead to almost null matrix elements for values of  $g_{pp}$  in its physical range. The great sensitivity of  $M_{GT}^{2\nu}$  on  $g_{pp}$  makes difficult to make definite rate prediction, contrary to the Shell Model case. The value of  $g_{pp}$  has to be adjusted, otherwise the QRPA rates span a wide range of values. On the contrary, the  $(2\beta)0\nu$  rates are not so sensitive. The neutrino potential makes the difference with the  $(2\beta)2\nu$  case. The various multipolarities (besides  $J^\pi = 1^+$ ) arising because of its radial dependence, wash out much of the suppression. The nuclear sensitivity of the  $0\nu$  rates is rather smooth and the predictions are much more reliable. The QRPA has been applied to most of the  $2\beta$  emitters.

Several QRPA variants (like the Multiple Commutator Method, MCM [17]) or extensions have been also applied, as well as some alternative methods, like the Operator Expansion Method (OEM) [18], the SU(4) symmetry, the  $1^+$  intermediate state dominance model ( $1^+\text{D}$ ) [19], the pseudo SU(3), and quite a few more (see Ref. [17] for a recent theoretical review). The OEM, for instance, which avoids summation over intermediate states, predicted results much less sensitive to  $g_{pp}$ , but has also several drawbacks. The alternative  $1^+\text{D}$  model of Zaragoza/Osaka [19,7], suggested a long time ago [19], relies on the fact that in a double beta transition, the intermediate state (odd-odd nucleus) having  $1^+$  ground state (gs) can decay by EC to the initial gs, and by  $\beta^-$  to the gs of the final nucleus and so the feeding of pertinent ft-values provide the  $2\beta$  decay nuclear matrix elements. An archetypical example is provided by the transition  $^{100}\text{Mo}$ – $^{100}\text{Tc}$ – $^{100}\text{Ru}$ , which in most of the calculations is predicted to decay faster than observed ( $\sim 10^{19}$  y). The QRPA did not work either for  $^{100}\text{Mo}$ , nor did some of their cures like the OEM (almost insensitive to  $g_{pp}$ ), which fall a factor three apart from the experimental value. However, by assuming a dominant contribution of the lowest state of the intermediate nuclei, the correct value of  $M_{2\nu}$  could be reproduced [20], as already noted quite a few years ago [19] in this and other transitions. Working out this model (i.e. feeding the single GT transition matrix element as given by experiment [say from  $\beta^-$  and EC decays and/or

Table 3

Neutrinoless half-lives in various Theoretical Models (for the  $\langle m_\nu \rangle$  Term)  $T_{1/2}^{0\nu} \langle m_\nu \rangle^2$  values are given in  $10^{24} (\text{eV})^2 \text{ y}$ .

	$^{76}\text{Ge}$	$^{82}\text{Se}$	$^{100}\text{Mo}$	$^{128}\text{Te}$	$^{130}\text{Te}$	$^{136}\text{Xe}$	$^{150}\text{Nd}$	$^{116}\text{Cd}$	$^{48}\text{Ca}$
Weak Coupl. SM [2,12]	1.67	0.58		4.01	0.16				
$g_A = 1.25(g_A = 1)$	(3.3)	(1.2)		(7.8)	(0.31)				
Large Space SM [13]	17.5	2.39				12.1			6.25
QRPA [14]	14	5.6	1.9	15	0.66	3.3			
QRPA [16]	2.3	0.6	1.3	7.8	0.49	2.2	0.034	0.49	
QRPA [15]	2.15	0.6	0.255	12.7	0.52	1.51	0.045		
OEM [18]	2.75	0.704		12.6	0.723	4.29	0.056	0.583	
QRPA with	18.4	2.8	350	150	2.1	2.8		4.8	28
(without) np pair. [22]	(3.6)	(1.5)	(3.9)	(19.2)	(0.86)		(4.7)	(2.4)	

(pn),(np), ( $^3\text{He}$ ,t) reactions, presently being carried out at RCNP (Osaka)], Ejiri et al. obtained  $2\beta 2\nu$  half-life values in fair agreement with the experiment [6,21].

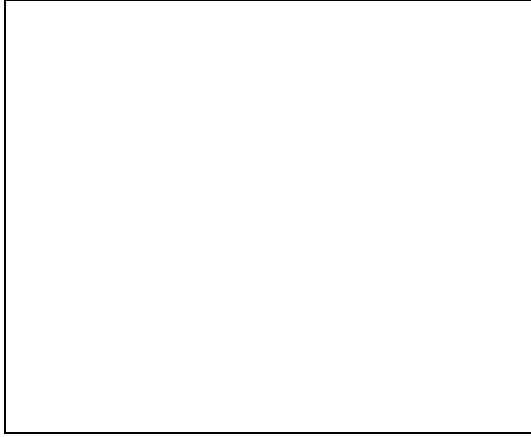


Figure 8.

Results of  $2\nu$  and  $0\nu$  theoretical half-lives are given in Tables 1 and 3 according to various nuclear models. The reader can derive by himself from Tables 3 and 2 the  $\langle m_\nu \rangle$  upper bounds according to his preferred nuclear model. Figure 8 summarizes the confrontation theory vs. experiment in the two-neutrino decay modes, whereas

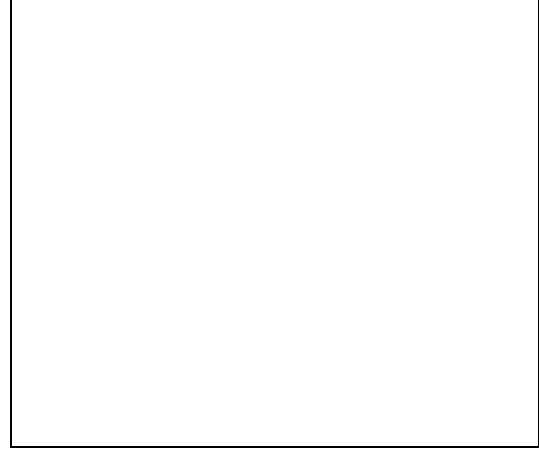


Figure 9.

Figure 9 gives a comparison of the neutrinoless half-life results of the various major experiments, and the corresponding neutrino mass bounds. The white hystograms represent the half-life limit each experiment must reach to match the current bounds for the neutrino mass obtained in germanium experiments.

## 5. CONCLUSIONS AND OUTLOOK

The standard  $2\beta 2\nu$  decay has been directly observed in several nuclei:  $^{48}\text{Ca}$ ,  $^{76}\text{Ge}$ ,  $^{82}\text{Se}$ ,  $^{96}\text{Zr}$ ,

$^{100}\text{Mo}$ ,  $^{116}\text{Cd}$  and  $^{150}\text{Nd}$  and others are under investigation ( $^{130}\text{Te}$ ,  $^{136}\text{Xe}$ ). QRPA reproduces reasonably well the measured half lives with some fine tuning of the nuclear parameter. Recent (large model space) shell model calculations give also good predictions in the cases where they have been applied so far, reinforcing the confidence on the matrix elements needed to extract the experimental limits on  $2\beta 0\nu$  decay. Data from the most sensitive experiments on  $2\beta 0\nu$  lead to the limit  $< m_\nu > < 0.4 - 1.5 \text{ eV}$  for the effective neutrino mass, according to the nuclear model.

The Ge experiments provide the stringest bound to the neutrino mass parameter and they seem to offer, for the next future, the best prospectives to reach the lowest values of  $< m_\nu >$ . The Heidelberg-Moscow experiment and IGEX on  $^{76}\text{Ge}$  will continue the data taking with a background reduced by pulse shape discrimination. These experiments will achieve sensitivities of order  $T_{1/2}^{0\nu} \approx 5 \times 10^{25} \text{ y}$  or close to  $10^{26}$  in  $^{76}\text{Ge}$ , corresponding to  $< m_\nu > \approx 0.2 - 0.6 \text{ eV}$  (according to the nuclear matrix element used). As proved by the 20-crystal array bolometers of the Milan group, the low temperature thermal detection of  $2\beta$  decays is now mastered. The cryogenic detectors are supposed to provide better energy resolution and more effective absorption of the particle energy (thermal vs ionization) and so the CUORE project is a promising (and feasible) undertaking.

Summarizing, currently running or planned experiments (H/M, IGEX, NEMO 3, MUNU, Bolometer Arrays), will explore effective neutrino masses down to about 0.1—0.3 eV. To increase the sensitivity it is necessary to go to larger source masses and reduce proportionally the background. That would bring the sensitivity to neutrino mass bounds below the tenth of electronvolt. Projects like CUORE [11] or GENIUS [4] go in that direction. To pursue the goal even further, huge detector masses, and still better event identification are needed.

In spite of the progress, a long way is still ahead of us. What is at stake is worth the effort.

## 6. ACKNOWLEDGEMENTS

I am indebted to my colleagues of the IGEX Collaboration, in particular to J. Morales for discussion and comments, and to CICYT (Spain) and the Commission for Cultural, Education and Scientific Exchange between the United States of America and Spain for financial support.

## REFERENCES

1. J. Schechter, J.W.F. Valle, Phys. Rev. D 25 (1982) 2951.
2. W.C. Haxton, G.J. Stephenson Jr., Prog. Part. Nucl. Phys. 12 (1984) 409.
3. M. Doi, T. Kotani, E. Takasugi, Progr. Theor. Phys. Suppl. 83 (1985) 1.
4. H.V. Klapdor, these Proc. and Refs. therein.
5. A. De Silva et al., Phys. Rev. C56 (1997) 2451, and A. Balysh et al., Phys. Rev. Lett. 77 (1996) 5186.
6. F. Piquemal, these Proc. and Refs. therein.
7. H. Ejiri, these Proc. and Refs. therein.
8. J-C. Vuilleumier et al., Phys. Rev. D48 (1993) 1009, and J. Farine, Proc. Neutrino 96, Helsinki, June 1996. Ed. K. Enqvist et al., World Scientific, p. 347.
9. V. Artemiev et al., Phys.Lett.B345(1995)564.
10. F. Danevich et al., Phys.Lett.B344(1995)72.
11. O. Cremonesi, these Proc. and Refs. therein.
12. W.C. Haxton, Nucl. Phys. B (Proc. Suppl.) 31 (1993) 82 and Refs. therein.
13. a) E. Caurier et al., Phys. Lett. B 252 (1990) 13 and Erratum, Phys. Rev. C 50 (1994) 223.  
b) E. Caurier et al., Phys. Rev Lett. 77 (1996) 1954; J. Retamosa et al., Phys. Rev. C 51 (1995) 371; A. Poves et al., Phys. Lett. B 361 (1995) 1.
14. P. Vogel and coll., Phys. Rev. Lett. 57 (1986) 3148; Phys. Rev. C 37 (1988) 731. See also M. Moe and P. Vogel, Ann. Rev. Nucl. Part. Sci. 44 (1994) 247.
15. A. Faessler and coll., Phys. Lett. B 194 (1987) 11; B 199 (1987) 473. See also T. Tomoda, Rep. Prog. Phys. 54 (1991) 53.
16. A. Staudt et al., Europhys. Lett. 13 (1990) 31 and Refs. therein.
17. J. Suhonen et al., Phys. Rep. 300 (1998) 123.

18. X.R. Wu et al., Phys. Lett. B 272 (1991) 169 and B 276 (1992) 274 and J. G. Hirsch et al., Nucl. Phys. A 589 (1995) 445.
19. J. Abad, A. Morales, R. Núñez-Lagos, A.F. Pacheco, Ann. Fis. A 80 (1984) 9; J. Phys. C3 Suppl. 45 (1984) 147.
20. A. Griffiths and P. Vogel, Phys. Rev. C 47 (1993) 2910.
21. H. Ejiri, Int. J. of Mod. Phys. E 6 (1997) 1.
22. G. Pantis et al., Phys. Rev. 53 C (1996) 695.
23. B. Kayser et al., "New and Exotic Phenomena", Ed. O. Facker, Editions Frontieres 1987, p. 349.

